

Preparation and characterization of flexible and elastic porous tubular PTMC scaffolds for vascular tissue engineering

Z. Guo^a, D. W. Grijpma^{a,b,c} and A. A. Poot^{a,c,*}

Vascular grafts with an inner diameter less than 6 mm are urgently needed due to the increasing prevalence of vascular disease. In this study, tubular scaffolds for vascular tissue engineering were fabricated by photo-crosslinking of acrylate-functionalized poly(trimethylene carbonate) (PTMC) macromers of different molecular weights in a glass mold. Porous structures were prepared by means of salt leaching. Tubular scaffolds were obtained with an inner diameter of 3 mm, a wall thickness of 1 mm, and a length of 4.5 cm. Pore sizes ranged from 0 to 290 μm , and the porosity was around 70%. The pores were homogeneously distributed and interconnected. PTMC macromers with a molecular weight of 4, 8, 13, 17, and 22 kg/mol were used. With increasing PTMC macromer molecular weight from 4 to 22 kg/mol, the E-modulus and maximum tensile strength of the scaffolds in the radial direction increased from 0.56 to 1.12 MPa and 0.12 to 0.55 MPa, respectively. Stress-strain curves for scaffolds made of 13, 17, and 22 kg/mol PTMC macromers showed a "toe" region characteristic for native arteries, followed by a linear increase until the maximum stress was reached. The E-moduli of the latter scaffolds are comparable to those of native arteries, whereas the maximum tensile strengths are approximately fourfold lower. This can be improved, however, by cell seeding in the porous scaffolds and subsequent mechanical stimulation in a bioreactor. It is concluded that the porous tubular scaffolds made of 13, 17, and 22 kg/mol PTMC macromers are suitable scaffolds for vascular tissue engineering. Copyright © 2016 John Wiley & Sons, Ltd.

Keywords: small-diameter vascular graft; poly(trimethylene carbonate); photo-crosslinking; glass mold; salt leaching

INTRODUCTION

Peripheral vascular disease is in most cases related to narrowing or occlusion of arteries and affects 12 to 20% of the population older than 65 years.^[1] Peripheral vascular disease can be treated by placement of a bypass graft, for which purpose autologous blood vessels, allografts, xenografts, or synthetic grafts of Dacron or Teflon are being used. These have all limitations such as low availability, immune responses, and low patency rates,^[2] which may be overcome by vascular tissue engineering.

The purpose of vascular tissue engineering is to produce tubular grafts with similar properties as the native blood vessels that should be replaced.^[3] Current strategies to fabricate such grafts include scaffold-guided tissue engineering and scaffold-free approaches such as assembly by cell sheet technology and 3D bioprinting.^[4–6] In view of the required mechanical properties of the grafts, design considerations as well as relatively low costs, a large amount of research has focused on scaffold-guided tissue engineering.^[7] In addition to the use of biocompatible materials and reproducible fabrication methods, the scaffold must have an appropriate structure for the intended application, be sufficiently strong to bear forces *in vivo*, and promote cell attachment and growth of new tissue. To fulfil the latter requirement, the scaffold should consist of an interconnected porous structure.^[8]

Porous tubular scaffolds can be prepared by combined solvent casting on a rod and particulate leaching, electrospinning on a rotating rod, and 3D printing of designed structures.^[9–11] Although solvent casting of a polymer solution containing

leachable particles is feasible,^[9] this method has a relatively low consistency in terms of wall thickness of the scaffold. Although electrospinning is a popular technique for the fabrication of tissue engineering scaffolds, these may suffer from poor cell penetration due to small pore sizes and poor control over mechanical properties.^[10] 3D printing is a promising technique to be applied in vascular tissue engineering. Not all polymers, however, are appropriate for 3D printing, and scaffolds may have unsuitable mechanical properties.^[12] Thus, the development of a new method to fabricate suitable porous tubular scaffolds for vascular tissue engineering is imperative.

* Correspondence to: André A. Poot, MIRA - Institute of Biomedical Technology and Technical Medicine and Department of Biomaterials Science and Technology, Faculty of Science and Technology, University of Twente, PO Box 217, 7500 AE Enschede, the Netherlands.
E-mail: a.a.poot@utwente.nl

a Z. Guo, D. W. Grijpma, A. A. Poot
MIRA - Institute of Biomedical Technology and Technical Medicine and Department of Biomaterials Science and Technology, Faculty of Science and Technology, University of Twente, PO Box 217, 7500, Enschede, the Netherlands

b D. W. Grijpma
W.J. Kolff Institute, Department of Biomedical Engineering, University Medical Centre Groningen, University of Groningen, PO Box 196, 9700, Groningen, the Netherlands

c D. W. Grijpma, A. A. Poot
Collaborative Research Partner, Annulus Fibrosus Rupture Program of AO Foundation, Davos, Switzerland

In view of its biocompatibility, biodegradability, and rubber-like mechanical properties, poly(trimethylene carbonate) (PTMC) is an excellent polymer for tissue engineering applications. Acrylate-functionalized PTMC macromers can easily be processed and photo-crosslinked for the preparation of scaffolds.^[13] Salt leaching has widely been used to create porous structures.^[14] In this study, we investigated the preparation of porous tubular scaffolds for vascular tissue engineering by means of photo-crosslinking of acrylate-functionalized PTMC macromers in a glass mold combined with salt leaching.

EXPERIMENTAL

Materials and equipment

Trimethylene carbonate (1,3-dioxane-2-one, TMC) was provided by Huizhou Foryou Medical Devices (Shenzhen, China). 1,1,1-Tris(hydroxymethyl)propane (trimethylolpropane) was purchased from Fluka. Tin (II) ethylhexanoate [Sn(Oct)₂], hydroquinone, methacrylic anhydride (MA), trimethylamine, and Irgacure 2959 were obtained from Sigma-Aldrich. Propylene carbonate (PC) and calcium hydride were ordered from Merck Millipore. Dichloromethane and ethanol (99.8%) were bought from VWR Chemicals. Dichloromethane was dried by calcium hydride and distilled under argon atmosphere. Salt particles were sieved to a size of 250 to 425 μm by using stainless steel sieves and subsequently dried in an oven at 120°C for 2 days. The glass mold consisted of two quartz glass tubes with different diameters, which were custom ordered from Technical Glass Products (Painesville, USA). MilliQ water was prepared by a Millipore Advantage A10 from Merck Millipore.

PTMC-MA synthesis and formulation of PTMC-MA/PC/salt resin

Three-armed PTMC was synthesized by ring-opening polymerization of TMC, using Sn(Oct)₂ as catalyst and trimethylolpropane as initiator, under argon at 130°C for 2 days. PTMC molecular weight was controlled by varying the amount of initiator. Three-armed PTMC was subsequently converted to PTMC-MA macromer as described by Geven *et al.*^[13] Three-armed PTMC oligomer and PTMC-MA macromer were analyzed by ¹H-NMR (Bruker Ascend 400/Avance III 400 MHz NMR spectrometer) to determine the average molecular weight (*M_n*), conversion of TMC, and degree of functionalization with MA.

Photo-crosslinkable resin was prepared by dissolving PTMC-MA macromer in PC for 2 days, after which Irgacure 2959 (2.5 wt% relative to PTMC-MA) was added as photo-initiator under stirring for 1 hr. Subsequently, dried salt particles were added to the solution that was mixed by hand with a spoon. The weight ratio of PTMC-MA:PC:salt was 1:4:9.

Photo-crosslinking of PTMC-MA/PC/salt resin and post-processing

Annular glass molds with an inner and outer diameter of 5 and 8 mm, respectively, were filled with PTMC-MA/PC/salt resins containing 4, 8, 13, 17, or 22 kg/mol PTMC-MA. Pieces of plastic tube with an inner diameter of 5 mm and a wall thickness of 1.5 mm were used as stoppers. UV crosslinking was carried out for 30 min at 365 nm in an UltraLum crosslinking cabinet. In order to obtain homogeneous crosslinking and to keep a homogeneous distribution of the salt particles, the molds were turned 6 times for 180°.

After cooling to room temperature, the inner tube of the mold could be easily removed. To remove the outer tube of the mold, the photo-crosslinked structure was soaked for 2 days in a PC/ethanol solution (3:7, v/v). Subsequently, the PC was removed by extraction of the structures in a graded series of PC/ethanol solutions, starting at a ratio of 8:2 until 0:10 (v/v). The extraction solutions were refreshed daily. After extraction, the solid structures containing ethanol were dried at 50°C for 12 hr. Finally, the salt particles were leached from the tubes by soaking for 2 days in MilliQ water. After rinsing with ethanol, the porous tubular crosslinked PTMC scaffolds were dried at 30°C for 2 days under vacuum. A schematic representation of the fabrication method is shown in Fig. 1.

Characterization of porous tubular PTMC scaffolds

The porosity of the tubular crosslinked PTMC scaffolds was determined gravimetrically according to eqn 1,

$$\text{Porosity} = [1 - (W_{\text{dry}} / V_{\text{dry}} \cdot \rho_{\text{PTMC}})] \cdot 100\% \quad (1)$$

in which $\rho_{\text{PTMC}} = 1.34 \text{ g/cm}^3$, W_{dry} is the dry weight of the scaffold, and V_{dry} is the volume of the scaffold in dry condition (regarded as a solid tube).

The pore size distribution of the tubular crosslinked PTMC scaffolds was determined by scanning electron microscopy (SEM), using a Hitachi S800 operating at 5 kV. Prior to imaging, dry specimens were coated with gold-platinum by using a Polaron E5600 sputter coater.

Micro-computed tomography (Micro-CT) was used to obtain a three-dimensional visualization of the pore structures of the scaffolds. A General Electric Explore Locus SP was used operating at 90 kV and 80 μA. The resolution was 14 μm. Average pore size and porosity were calculated from the data generated with scaffolds in dry condition.

The tensile properties of dry porous tubular crosslinked PTMC scaffolds were determined in the radial direction according to standards of the American National Standards Institute and the Association for the Advancement of Medical Instrumentation (ANSI/AAMI VP20: 1994) at a pulling rate of 1 mm/min, using a

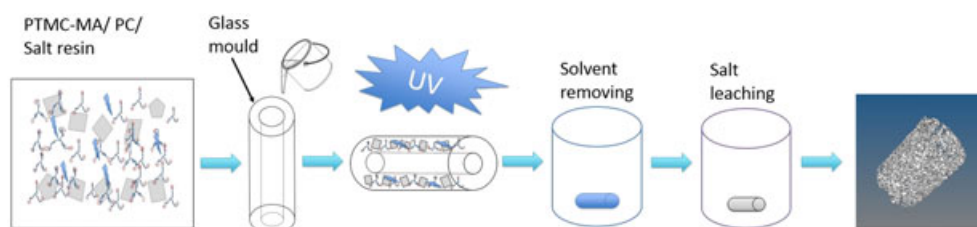


Figure 1. Schematic representation of the preparation of porous tubular crosslinked PTMC scaffolds.

Table 1. Characterization of the three-armed PTMC-MA macromers

	4 k	8 k	13 k	17 k	22 k
PTMC macromer molecular weight (M_n)	4500 g/mol	8000 g/mol	13600 g/mol	17000 g/mol	22300 g/mol
Monomer conversion	99.8%	99.8%	99.6%	99.3%	99.4%
Degree of functionalization	96%	92%	87%	91%	93%

Intended molecular weights are abbreviated as 4, 8, 13, 17, and 22 k.

Zwick Z020 tensile tester. The initial stiffness was determined from the slope of the tensile curve between 5 and 15% of strain.

RESULTS AND DISCUSSION

Characterization of PTMC-MA

The average molecular weight (M_n) of the three-armed PTMC oligomers, conversion of TMC monomer, and degree of functionalization of the oligomers with MA are shown in Table 1. All monomer conversions were higher than 99%, and the molecular weights of the PTMC oligomers were close to the intended values. The degree of functionalization of the oligomers with MA ranged from 87 to 96%, indicating that all PTMC macromers contained enough double bonds for efficient crosslinking.

Characterization of porous tubular crosslinked PTMC scaffolds

Physical parameters of the scaffolds

Figure 2 shows the glass mold used for the preparation of the crosslinked PTMC scaffolds as well as a macroscopic picture of one of the tubes after de-molding and post-processing. The annular space of the mold had an inner and outer diameter of 5 and 8 mm, respectively. The inner and outer diameters of the tubular PTMC scaffolds, however, were smaller. As shown in Table 2, the scaffolds had an inner diameter around 3 mm and a wall thickness of approximately 1 mm (*i.e.* an outer diameter of 5 mm). This difference can be explained by shrinkage of the

scaffolds during post-processing. Photo-crosslinking of the PTMC-MA macromers took place in the swollen state, due to the presence of PC, resulting in contraction of the PTMC network upon extraction of PC and subsequent salt leaching. Also, the length of the scaffolds decreased, from approximately 7 cm after photo-crosslinking in the mold to 4.5 cm after post-processing (data not shown).

As shown in Table 2, the porosities of the scaffolds as determined by gravimetry amounted to approximately 75%. The theoretical porosity based on the volume ratio of salt to PTMC was 83%. This discrepancy can also be explained by shrinkage of the structures during extraction and salt leaching. Porosities determined by Micro-CT were around 67% (Table 2). This is lower than the gravimetric data, probably because of the Micro-CT resolution of 14 μm .

The average pore size of the scaffolds as determined by Micro-CT was approximately 87 μm . Micro-CT imaging showed that the pores were homogeneously distributed throughout the scaffolds (Fig. 3). Pore sizes determined by SEM ranged from 0 to 290 μm (Table 2). This is smaller than the sizes of the salt particles (250–425 μm), again due to shrinkage of the structures during post-processing. SEM imaging showed that both the outer and inner surfaces of the wall of the scaffolds had an open porous structure (Fig. 4). Moreover, cross-sections of the scaffolds showed that the pores were interconnected. As reported by Yannas, human aortic smooth muscle cells in suspension have a length and diameter of approximately 55 and 8 μm , respectively, and the optimal pore size for migration of the cells through a scaffold is around 100 μm .^[15] Thus, the pore characteristics of the scaffolds meet the requirements for successful cell seeding and migration.

Table 2 also shows that the dimensions, porosities, and pore sizes of the crosslinked 4 and 8 k PTMC scaffolds were lower than those of the scaffolds prepared with the higher molecular weight PTMC-MA macromers. The reason for this is that the crosslinked 4 and 8 k PTMC scaffolds shrunk more during extraction because of the shorter chain lengths between crosslinks and thus a higher crosslink density. Finally, Table 2 shows comparable physical parameters of porous tubular PTMC scaffolds (B50) fabricated by Song *et al.*, by casting of high molecular weight linear PTMC/salt suspension on a glass rod, followed by crosslinking by means of γ -irradiation and leaching of the salt particles in water.^[9] As those PTMC scaffolds proved to be very suitable for vascular tissue engineering, this can also be expected for the scaffolds prepared in the present study.

Mechanical properties of the scaffolds

For application in vascular tissue engineering, the mechanical properties of the scaffolds are very important. After seeding of cells, e.g. smooth muscle cells or stem cells, in the pores of the scaffolds, subsequent mechanical stimulation in a

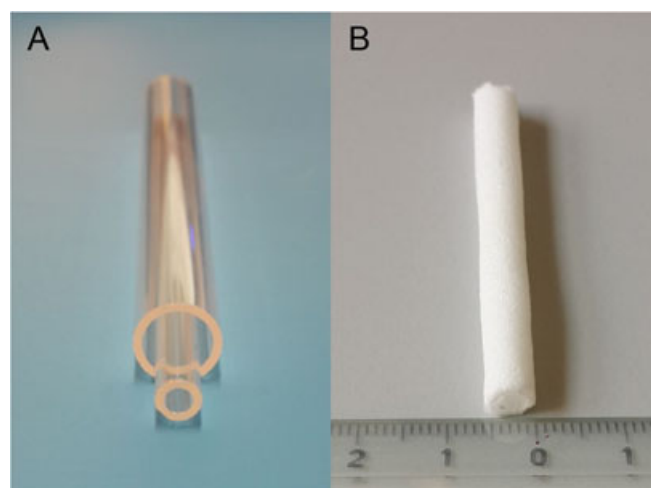


Figure 2. Glass mold (A) and macroscopic appearance of a porous tubular crosslinked PTMC scaffold after salt leaching (B).

Table 2. Physical parameters of porous tubular crosslinked PTMC scaffolds

Parameters	4 k	8 k	13 k	17 k	22 k	B50 ^a
Inner diameter ^b , mm	2.96 ± 0.06	3.00 ± 0.06	3.12 ± 0.09	3.16 ± 0.8	3.18 ± 0.8	3.15 ± 0.28
Wall thickness ^b , mm	0.95 ± 0.04	0.98 ± 0.04	1.04 ± 0.04	1.05 ± 0.04	1.07 ± 0.04	0.83 ± 0.25
Porosity ^c , vol%	73 ± 2.1	73 ± 2.6	75 ± 4.3	76 ± 3.3	77 ± 3.1	82.2 ± 2.0
Porosity ^d , vol%	61 ± 3.2	64 ± 2.3	67 ± 2.1	69 ± 1.2	68 ± 2.6	77.8 ± 1.7
Average pore size ^d , μm	81	81	87	91	93	108
Pore size range ^e , μm	0–280	0–283	0–286	0–294	0–289	0–308

^aPorous tubular PTMC scaffold prepared by Song *et al.* by dip coating, crosslinking by γ -irradiation, followed by salt leaching.^[9]
^bInner diameter and wall thickness of all porous tubular PTMC scaffolds were measured by using a caliper.
^cPorosity as determined by gravimetry.
^dPorosity and average pore size as determined by Micro-CT.
^ePore size range as determined by SEM.

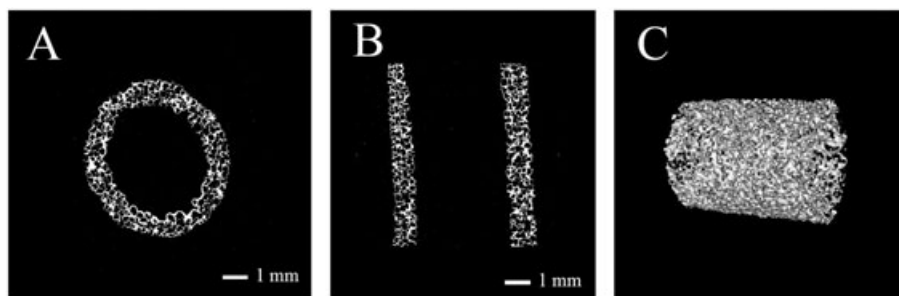


Figure 3. Micro-CT images of a porous tubular crosslinked PTMC scaffold. Transversal cross-section (A), longitudinal cross-sections (B), and generated 3D image (C).

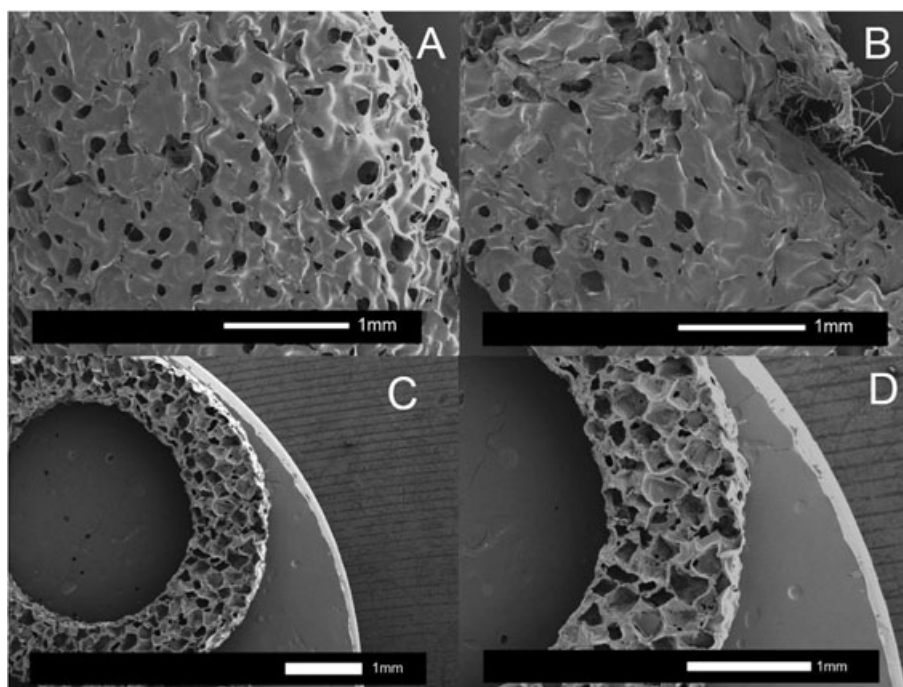


Figure 4. SEM images of a porous tubular crosslinked PTMC scaffold. Outer surface (A), inner surface (B), and cross sections (C) and (D).

Table 3. Tensile properties of porous tubular crosslinked PTMC scaffolds and natural arteries in the radial direction

Sample	Initial stiffness, MPa	Maximum tensile strength, MPa	Elongation, %
4k	0.56 ± 0.09	0.12 ± 0.05	382 ± 40
8k	0.53 ± 0.06	0.25 ± 0.03	820 ± 60
13k	0.79 ± 0.09	0.32 ± 0.03	1130 ± 150
17k	0.89 ± 0.12	0.41 ± 0.04	1320 ± 180
22k	1.12 ± 0.30	0.55 ± 0.03	1080 ± 160
B-50 ^a	1.10 ± 0.08	0.17 ± 0.04	1214 ± 120
Ovine carotid artery ^a	1.21 ± 0.14	1.65 ± 0.08	255 ± 21
Human arteria mesenterica inferior ^a	5.7	1.89	345

^aData from Song *et al.*^[9] B-50 refers to a porous tubular PTMC scaffold prepared by dip coating, crosslinking by γ -irradiation, followed by salt leaching.

bioreactor is most effective when the mechanical properties of the constructs comply with those of native arteries. This especially holds for the mechanical properties in radial direction. The pulsatile flow of blood *in vivo* causes cyclic distension of the arterial wall, which in turn affects cell differentiation, function, and orientation.

As shown in Table 3, the initial stiffness (E-modulus) and maximum tensile strength in the radial direction of the porous tubular crosslinked scaffolds increased from 0.56 to 1.12 MPa and 0.12 to 0.55 MPa, respectively, with increasing PTMC-MA macromer molecular weight from 4 to 22 kg/mol. The increasing tensile strength with increasing macromer molecular weight is in agreement with data reported by Schüller-Ravoo *et al.* for photo-crosslinked PTMC network films.^[16] In the latter study, however, the E-modulus decreased with increasing PTMC-MA macromer molecular weight from 3 to 24 kg/mol. Using 3k macromer, densely crosslinked brittle films were obtained, whereas 18, 20, and 24k macromers yielded rubber-like elastomeric films. It should be noted that the scaffolds in the present study were porous. Increasing porosity decreases the mechanical properties of scaffolds, especially the E-modulus. As the porosities of the tubular crosslinked PTMC scaffolds were the same, this cannot explain the lower E-moduli of the scaffolds prepared with the lower

molecular weight macromers. Most likely, this was caused by the processing conditions that were used. The tubular PTMC scaffolds were crosslinked in the presence of the non-reactive diluent PC and salt particles. Upon extraction of the PC, the brittle networks formed with the lower molecular weight macromers may have been partially damaged because of contraction while the salt particles were still in place. Subsequent salt leaching resulted in porous scaffolds with lower E-moduli.

The number of acrylate groups available for photo-crosslinking decreased with increasing PTMC-MA macromer molecular weight. Because of this and the relatively large amount of non-reactive diluent present in the resins, it was expected that the efficiency of photo-crosslinking would decrease with increasing PTMC-MA macromer molecular weight. Indeed, crosslinked scaffolds could not be formed using macromers with a molecular weight higher than 22 kg/mol.

Whereas the E-modulus of the 13, 17, and 22k scaffolds was comparable to that of the B50 scaffold previously prepared by Song *et al.*,^[9] the maximum tensile strength of the scaffolds prepared in the present study was higher. Stress-strain curves for the 13, 17, and 22k scaffolds showed a “toe” region characteristic for native arteries, followed by a linear increase until the maximum stress was reached^[17] (Fig. 5). Elongations at break were higher than 1000%. The E-moduli of the 13, 17, and 22k scaffolds are comparable to those of native arteries, whereas the maximum tensile strengths are approximately fourfold lower (Table 3). This can be improved, however, by cell seeding in the scaffolds and subsequent mechanical stimulation as described earlier.

CONCLUSIONS

This study shows that photo-crosslinking of acrylate-functionalized PTMC macromers in a glass mold followed by salt leaching is a feasible method to prepare suitable scaffolds for vascular tissue engineering. Although the tubular crosslinked PTMC scaffolds shrink during post-processing, this can be taken into account during fabrication. Desired scaffold dimensions can be obtained by adjusting the dimensions of the mold. In view of their mechanical properties, porous tubular scaffolds made of PTMC macromers with a molecular weight of 13–22 kg/mol are the preferred scaffolds for vascular tissue engineering.

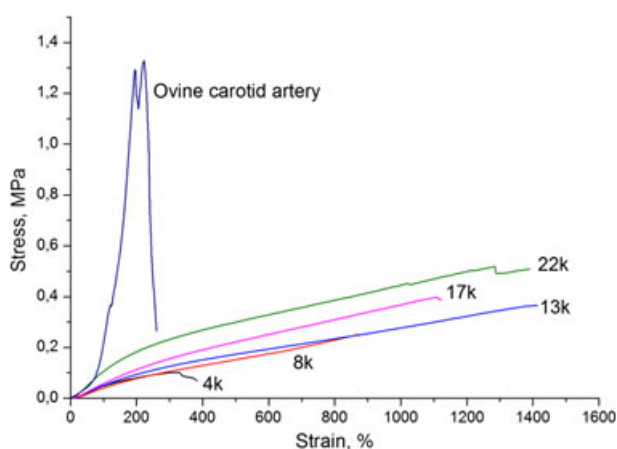


Figure 5. Stress-strain measurements of the porous tubular crosslinked PTMC scaffolds and an ovine carotid artery.

Acknowledgements

The authors would like to thank the China Scholarship Council for financial support.

CONFLICT OF INTEREST

The authors have no conflicts of interest to declare.

REFERENCES

- [1] <http://www.healthline.com/health/peripheral-vascular-disease>
- [2] P. Zilla, D. Bezuidenhout, P. Human, *Biomaterials* **2007**, *28*, 5009.
- [3] D. G. Seifu, A. Purnama, K. Mequanint, D. Mantovani, *Nat. Rev. Cardiol.* **2013**, *10*, 410.
- [4] A. Patel, B. Fine, M. Sandig, K. Mequanint, *Cardiovasc. Res.* **2006**, *71*, 40.
- [5] N. L'Heureux, S. Paquet, R. Labbe, L. Germain, F. A. Auger, *FASEB J.* **1998**, *12*, 47.
- [6] C. Norotte, F. S. Marga, L. E. Niklason, G. Forgacs, *Biomaterials* **2009**, *30*, 5910.
- [7] J. D. Berglund, Z. S. Galis, *Br. J. Pharmacol.* **2003**, *140*, 627.
- [8] I. Martin, D. Wendt, M. Heberer, *Trends Biotechnol.* **2004**, *22*, 80.
- [9] Y. Song, M. M. J. Kamphuis, Z. Zhang, L. M. T. Sterk, I. Vermes, A. A. Poot, J. Feijen, D. W. Grijpma, *Acta Biomater.* **2010**, *6*, 1269.
- [10] A. Hasan, A. Memic, N. Annabi, M. Hossain, A. Paul, M. R. Dokmeci, F. Dehghani, A. Khademhosseini, *Acta Biomater.* **2014**, *10*, 11.
- [11] M. A. Cleary, E. Geiger, C. Grady, C. Best, Y. Naito, C. Breuer, *Trends Mol. Med.* **2012**, *18*, 394.
- [12] S. Baudis, F. Nehl, S. C. Ligon, A. Nigisch, H. Bergmeister, D. Bernhard, J. Stampfl, R. Liska, *Biomed. Mater.* **2011**, *6*, 055003.
- [13] M. A. Geven, D. Barbieri, H. P. Yuan, J. D. de Bruyn, D. W. Grijpma, *Clin. Hemorheol. Microcirc.* **2015**, *60*, 3.
- [14] D. W. Hutmacher, *J. Biomater. Sci. Polym. Ed.* **2001**, *12*, 107.
- [15] I. V. Yannas, *Adv. Polym. Sci.* **1995**, *122*, 219.
- [16] S. Schüller-Ravoo, J. Feijen, D. W. Grijpma, *Acta Biomater.* **2012**, *8*, 3576.
- [17] Y. C. Fung, Mechanical properties and active remodeling of blood vessels. In: *Biomechanics. Mechanical Properties of Living Tissues*. Springer, New York, **1993**.